Influence of H-D isotopic substitution on the protonic conductivity of $LiNbO_3$

S. Klauer, M. Wöhlecke, and S. Kapphan
Universität Osnabrück, Fachbereich Physik, Postfach 4469, D-4500 Osnabrück, Federal Republic of Germany
(Received 1 July 1991)

The electric dc dark conductivity in congruent $LiNbO_3$ has been studied in the temperature range 80–600 °C as a function of the proton and deuteron concentration and the driving electric field. The conductivity was found to follow an Arrhenius-like behavior with an activation energy equal for protons and deuterons, $\varepsilon_{act} = 1.23$ eV. The pre-exponential factor σ_0 shows a linear concentration dependence for both H and D, but with different slopes. The ratio of the slopes yields $(\partial\sigma_0/\partial c)_H/(\partial\sigma_0/\partial c)_D = 1.36$. This agrees with the mass dependence of the attempt frequencies in a hopping model of protons and deuterons and rules out models of OH-OD migration. The conductivity was found to be independent of the electric field up to values of 10^5 V/cm, which is comparable to inner electric fields in volume holograms in $LiNbO_3$. In the temperature range accessible to both methods, the dc and the holographically measured values of the conductivity agree very well, displaying the same temperature and concentration dependence. The charge-carrier concentration was determined from the integrated absorption strength of the ir OH-OD stretch-mode absorption of proton- and deuteron-exchanged waveguides with a known rate of exchange of Li by H-D, yielding an oscillator strength $f_H = 1.7 \times 10^{-2}$.

I. INTRODUCTION

The piezo- and electro-optical as well as the electrical properties of $LiNbO_3$ are considerably influenced by the presence of impurities like $3d$ ions and/or hydrogen. In crystals grown by the Czochralski method hydrogen is often present forming hydroxyl ions with oxygen. The incorporated hydrogen is assumed to be responsible for the reduction of photorefractive laser damage[1] and the thermal fixation of holograms in $LiNbO_3$. For the interpretation of the thermal fixation of holograms Amodei and Staebler[2] suggested that ions become mobile at elevated temperatures above 150 °C and compensate the modulated electronic space-charge fields built up during the writing process. As a result a hologram is produced, which is stable against erasure during read-out at room temperature.[2] These ions must be positively charged and by spatially resolved ir absorption were identified as protons.[3] In contrast to this, Bollmann assumes interstitial OH^- ion migration[4] and argues that OH^- ions at O^{2-} sites represent positive charges with respect to the unperturbed lattice.[5]

The fabrication of optical waveguides is another important field for applications of $LiNbO_3$. One possibility to produce waveguides can be realized by proton exchange during a treatment in benzoic acid at about 200 °C. Under these conditions a large amount of Li ions diffuses out of a surface layer, being partially replaced by protons, inducing a significant change in the extraordinary index of refraction.[6]

However, in spite of practical importance the microscopic mechanism of protonic migration and even the migrating species are not yet clear. The latter might be distinguished using the isotopic mass difference between protons and deuterons which influences the pre-exponential coefficient of diffusion and the associated electrical conductivity. The accuracy of previous diffusion experiments with protons, deuterons and even tritons did not allow a decision.[7,8] The protons present in the crystals are monitored via the ir absorption band of the OH stretching vibration. The intensity of this absorption band can be used as a measure for the content of protons in the crystal, if the appropriate oscillator strength is known. This calibration is necessary in order to derive the diffusion constant containing the physical parameters of the migration process from the measured electrical conductivity, which scales with the charge carrier density.

No data on the oscillator strength are available for the OD vibration in $LiNbO_3$. Values of the oscillator strength of the OH stretch mode vibrations in oxidic crystals vary by almost 2 orders of magnitude from about $f_H = 3.8 \times 10^{-2}$ for TiO_2 (Ref. 9) to $f_H = 1.2 \times 10^{-3}$ in $LiNbO_3$.[10] Less data are available for the different isotopic values of f_H and f_D, with the exception of a value $f_H/f_D \approx 1$ in TiO_2.[9] A determination of these data for the $LiNbO_3$ system under study is deemed to be necessary therefore.

The present work is intended to (i) expand the temperature range to the interval 100–200 °C, where both the conductivity can be measured *directly* and the thermal fixation of holograms is performed; (ii) link the conductivity data of the *direct* current measurements with those of the *indirect* access monitoring the thermal decay of holograms; (iii) provide similar experimental conditions in direct dc measurements and the thermal decay of holograms, concerning the strength of inner electric fields; (iv) decide on the migrating species (protons or hydroxyl ions) by an accurate determination of the isotope effect in the pre-exponential factor of the ionic conductivity;

(v) determine the oscillator-strengths of the OH and OD stretching vibration; (vi) correlate the ir absorption of the OH stretch mode with electrical conductivity.

II. EXPERIMENTAL INVESTIGATIONS

A. Preparation of samples

1. Preparation for dc-conductivity measurements

In order to achieve all of the above aims, we have measured the electrical dc dark conductivity as a function of temperature, driving electric field and proton and deuteron concentration. Thin plateletlike x-cut samples of size 10×11 mm^2 were cut from a 0.5-mm-thick wafer of congruent (48.6 mol% Li_2O), nominally pure $LiNbO_3$ purchased from Crystal Technology. The crystals were doped with protons or deuterons according to the following steps. The samples were sealed in platinum foil to prevent contamination and Li-out-diffusion and heated for 30 h at temperatures of 850 °C under O_2 atmosphere. This step was used to obtain proton concentrations below the "as grown" values by proton out-diffusion and to get defined starting conditions. Annealing the "as-grown" proton content was also necessary to suppress the protonic contribution to the electrical conductivity of the deuterium-doped samples. The method of electric field-enhanced in-diffusion[1] of protons or deuterons was used to raise the concentration. The samples were heated to about 600 °C in a humid atmosphere realized by evaporating H_2O or D_2O within a heated quartz rod. An electric field of about 400 V/cm was applied for about 20 min using silver paste electrodes covering the whole platelet area. In principle, the proton and deuteron content can be tuned by varying the temperature, the electric field and the switch-on time of the field. It turned out that a temperature of 600 °C resulted in optimum doping. For the actual dc-current measurements the samples were polished and Au electrodes were evaporated onto a thin Cr sublayer. At the ground side a closed guard-ring electrode was added to prevent the contribution of surface currents to the measurement.

2. Preparation for measurements of the oscillator strength of the OH/OD vibration

The aim of these experiments must be to measure the resultant ir absorption for known proton contents. One method to get rather defined proton concentrations is to produce proton-exchanged (PE) layers just as it is done in the fabrication of planar optical waveguides.[6]

The technique consists in treating $LiNbO_3$ in liquid proton-rich media, most usually benzoic acid (C_6H_5-COOH) at temperatures of about 240 °C for times in the range of several minutes to hundreds of hours. During this treatment protons diffuse into the crystal, replacing Li, which in turn diffuses out, one by one. A step-functionlike profile of protons is produced in the crystal, accompanied by a strong change Δn_e of the extraordinary index, a small change Δn_0 of the ordinary index of refraction[6] from the bulk values and an inverse profile for the Li concentration.[10–13] The degree of exchange of Li by H, called x, can be tuned by the acidity of the proton-rich melt and/or by adding Li salts to the melt. The addition of some mol% Li also prevents the usually polished crystal surfaces of $LiNbO_3$ from destruction.[12] For the measurements of waveguides modes, x-cut samples with optically polished surfaces were used. The samples were annealed at 850 °C before the proton exchange to suppress the bulk OH band. Most of the samples were proton exchanged in usual benzoic acid buffered with 1.5 mol% Li of Li benzoate. According to the linear relation of x with [Li] this treatment should result in $x = 0.70 \pm 0.05$.[11] Other samples were treated in fully deuterated benzoic acid (C_6D_5-COOD) with a specified isotopic pureness of 99.9% (VEB Berlin-Chemie, Berlin-Adlershof, GDR). Because no protons should be present in the melt, Li buffering was achieved with Li carbonate (Li_2CO_3). The temperature was kept constant at T=240 °C and the duration of the proton exchange was varied between 3.75 to 120 h to get layers of increasing thickness.

B. Optical methods for the determination of hydrogen and deuteron concentration

1. ir-absorption characterization

A FTIR spectrometer (Bruker model 113 cv) was used to record the well-known ir-absorption bands of the OH (3485 cm^{-1}) and the OD (2569 cm^{-1}) stretching vibration. All spectra were recorded at room temperature. In $LiNbO_3$ the bands are known to be perfectly polarized perpendicular to the c axis, reflecting the OH dipoles vibrating parallel to the respective oxygen planes. All absorption measurements reported here were done on x cuts, i.e., with the incident light beam perpendicular to the c axis. The linear polarized light was achieved by Perkin-Elmer wire grid polarizers.

Proton- and deuteron-exchanged (PE) platelets served as the calibration samples for the proton and deuteron content. The surface on the backside of the samples was ground so that only the protons in the waveguide on that side, which was investigated further, contributed to the absorption. The PE absorption bands of the protons and deuterons are slightly shifted relative to the bulk position from 3488 to 3508 cm^{-1} for OH and to 2592 cm^{-1} for OD. They show a more symmetric, flattened shape with an increase in their half-width for the samples used. The ir polarization behavior of the PE-absorption band must also be taken into account for a precise determination of the total OH-OD content. We found that the H-D PE bands are polarized perpendicular to the c axis as perfectly as the band caused by the protons incorporated into the bulk.

2. Waveguide characterization with a mode coupling method

The refractive index profile of the waveguides fabricated by PE can be reconstructed from the effective re-

fractive indices of guided modes. The modes were excited by the prism coupling method[14] using a He-Ne laser. For distinct angles of incidence energy can couple from the prism into the waveguide and excite a mode. This transverse resonance condition is fulfilled when the component of the wave vector of the incident beam in the direction of the waveguide equals one of the effective wave vectors of guided modes. This leads to a drop in the intensity of the laser beam emerging from the prism. For others than these resonance angles the beam is totally reflected at the prism-waveguide interface. The refractive indices belonging to the effective wave vectors can be calculated from these angles and the refractive indices of the air and the rutile prism. The modes propagated in the y direction perpendicular to the polar c axis. Consequently, the ordinary (Δn_o) and the extraordinary (Δn_e) refractive index profile can be determined separately . When the polarization of the incident light is perpendicular to the c axis, TM modes are excited. For polarization parallel the c axis, TE modes are guided. TE modes were excited because Δn_e is more pronounced than Δn_o. An improved version of the inverse WKB method[15] was used to reconstruct the profile of the refractive index change and to extract the thickness of the waveguide layer.

C. dc conductivity measurements

1. *Electric dc measurements*

The direct dc measurements of the electrical conductivity were performed with an electrometer (model Keithley 610 C). This instrument directly supplied the guarding potential applied to the guard electrode ring on the ground side of the samples. External voltages up to 2.5 kV were applied to avoid voltage break-throughs. A maximum electric field of 2×10^5 V/cm was reached with samples polished to 110 μm. The samples were held in an oven for stabilized temperatures between 100 and 600 °C with an accuracy of ±0.5 K. Au wires contacted the evaporated Au electrodes with silver paste. For sufficiently good electrical isolation, the Au wires were guided out of the high temperature region through quartz capillaries which themselves were held and isolated in a Teflon block at the low temperature end of the oven. All cables and the oven were carefully shielded. Current enhancing parameters (high voltage, large electrode areas, and thin samples) were selected to operate with expected signal currents exceeding the detection limit (10^{-14} A) of the electrometer by at least 2 orders of magnitude.

Below 100 °C the signal current began to oscillate very strongly. These fluctuations are attributed to displacement currents which may be comparable or even exceed the signal current, resulting from pyroelectric effects due to random temperature fluctuations of the sample.[16] In this temperature regime, the electric conductivity can be measured more accurately by indirect methods as listed by Blistanov,[17] or the holographic method.

2. *Holographic conductivity measurements*

To combine the direct dc measurements with the holographic results, two samples of $LiNbO_3$ (49.3 mol% Li_2O), co-doped with 660 mol ppm Fe, were prepared with a treatment and geometry similar to the samples used in the dc experiments. One sample was doped with protons to nearly precisely ten times higher content, the other left "as grown." The iron-doped crystal was supplied by the Siemens Research Laboratories, D-München (B. Grabmeier, crystal FE2). In the holographic method the decay with time of the diffraction efficiency of a sinusoidally modulated refractive index grating is recorded. The grating was inscribed into the crystals at room temperature by a two-beam interference using a single He-Ne laser beam split in two parts interfering within the sample.[18] The primary process is the formation of a modulated pattern of negative electronic space charges due to photoexcitation into the conduction band. Via the electro-optical effect this also modulates the index of refraction. Here in contrast to the experiments described above, we used Fe co-doped crystals to enhance the photoconductivity and the diffraction efficiency of the resulting gratings. When the temperature is elevated the protons become mobile and compensate the negative space-charge pattern. As a result, the diffraction efficiency decreases exponentially in time. After the samples had reached the desired temperature this decay was monitored recording the intensities of the diffracted and the transmitted beam for single beam illumination. Very low laser power was used to avoid a significant contribution of electronic photoconductivity. After the decay time measurement the crystals were homogeneously illuminated to erase the pattern and cooled down for the next cycle. In this way the temperature range 75–150 °C could easily be monitored. For higher temperatures the decay time decreases to some seconds so that the major decay happened already during the heating-up period thus preventing proper measurements. For the low temperatures the decay time became too long compared to the long-term stability of the experimental set-up operated at very low laser power.

III. EVALUATION OF DATA AND RESULTS

A. Calibration of the proton and deuteron concentration

In order to gauge the proton and deuteron concentration from the ir absorption we follow the definition given in the work of Johnson *et al.*[9] An "absorption strength per ion," $a_{\text{H-D}}$ is defined for the protons and deuterons by

$$a_{\text{H-D}} = \frac{A_{\text{int,H-D}}}{(\ln 10)c_{\text{H-D}}}, \tag{1}$$

where $c_{\text{H-D}}$ are the concentrations of the ions and

$$A_{\text{int,H-D}} = \int \alpha_{\text{H-D}}(\bar{\nu})d\bar{\nu} \tag{2}$$

are the integrated absorption constants for the OH and the OD bands, respectively. We determined the baseline of the spectrum as the straight line interpolating the flat background signal to the left and right of the band. The

baseline was subtracted from the spectrum and the peak was integrated to yield the value for A_{int}. Rule of thumb approximations of the form

$$A_{\text{int}} \approx \mathcal{F}\alpha_{\max}\Gamma \tag{3}$$

with the form factor $\mathcal{F}$ and the full width at half maximum Γ could not be applied here because of two reasons: The form factor $\mathcal{F}$ for the peaks is depending on starting material and composition of the samples used. Moreover the band shape of the OH bulk absorption is different from the OH bands of the PE layer at the surface. The absorption constant α is calculated according to

$$\alpha(\bar{\nu}) = \frac{D(\bar{\nu})\ln 10}{d}. \tag{4}$$

Here, $D(\bar{\nu})$ describes the optical density, the primary quantity yielded by an absorption spectrometer while d represents the thickness of the absorbing layer. The same relation also holds for the integrated optical density

$$D_{\text{int}} = \int D(\bar{\nu})d\bar{\nu} = \frac{A_{\text{int}}d}{\ln 10}. \tag{5}$$

The experimental uncertainty of the integrated optical density due to the difficulty in determining the baseline of the peaks was below 2%.

For the homogeneously doped samples d is simply the geometrical thickness of the crystal, while for the PE layers d is the average depth of the proton-concentration profile which was deduced from mode-coupling experiments. The extraordinary index change Δn_e is governed by the strongly increased proton concentration. The reconstructed index profiles of our waveguides are shown in Fig. 1. A constant value of Δn_e is followed by a sharp drop, which indicates a constant proton concentration or a homogeneous degree of exchange within the whole layer. This allows us to define the average depth d_{50} of the PE layer as the thickness, where the profile has decreased to 50% of its surface value. The maximum error $\Delta\ d_{50} = 0.05\ \mu$m reflects both, mechanical precision of the rotary stage and its influence on the reconstructed index profiles using the inverse WKB algorithm. The layer thickness d_{50} varied with the exchange time t_{ex} at constant temperature T_{ex}. In Fig. 2 we plotted the thickness d_{50} of the layers as a function of the square root of t_{ex}. A relation

$$d_{50} = 2\sqrt{D(T_{\text{ex}})t_{\text{ex}}}, \tag{6}$$

which is expected for a diffusion limited process, is perfectly satisfied.

The slopes of the resulting straight lines allow to define the effective diffusion constant $D(T_{\text{ex}})$ for the penetration of the exchange front. They are almost equal for the protons and deuterons: At 240 °C $D_{\text{H}} = (0.031\pm0.002)\mu^2/h$ and $D_{\text{D}} = (0.029\pm0.001)\mu^2/h$. We obtained good agreement with the data reported by Jackel *et al.*,[6] when taking into account the influence of M=1.5 mol% Li added to the melt, using the relation

$$D(M\%)/D(0\%) = 10^{-1.184M\%},$$

reported by Rottschalk (1988) for 250 °C.[12] The almost equal slopes in Fig. 2 result in a ratio $D_{\text{H}}/D_{\text{D}} = 1.069$, which is significantly smaller than expected for pure protonic and deuteronic diffusion. In this case it would be governed by the mass ratio $D_{\text{H}}/D_{\text{D}} = \sqrt{2} = 1.414$, as discussed below. This seems to indicate that the Li $\leftrightarrow$ H counterdiffusion process is governed by the mobility of the Li ions.

According to Eq. (5) the optical density should increase linearly with the layer thickness d_{50}. The optical densities for all samples investigated are plotted in Fig. 3 indicating the expected linear relation.

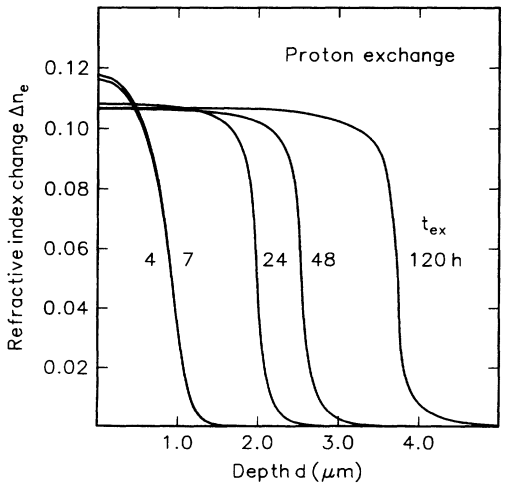

FIG. 1. Reconstructed profiles of the refractive index change Δn_e for the proton-exchanged waveguides, fabricated in benzoic acid buffered with 1.5 mol% Li benzoate at T_{ex} = 240 °C.

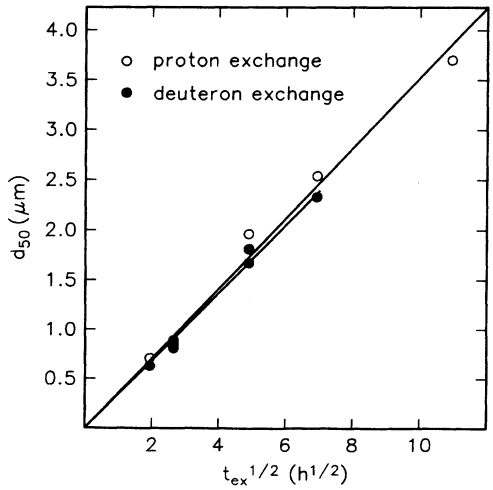

FIG. 2. PE-layer thickness d_{50} for proton- and deuteron-exchanged waveguides, plotted versus the square root of the exchange times t_{ex}. The two linear regression lines yield the effective diffusion constants D_{eff} for the penetration of the exchange front for the protons and deuterons, respectively, at T_{ex} = 240 °C in benzoic acid buffered with 1.5 mol% Li benzoate.

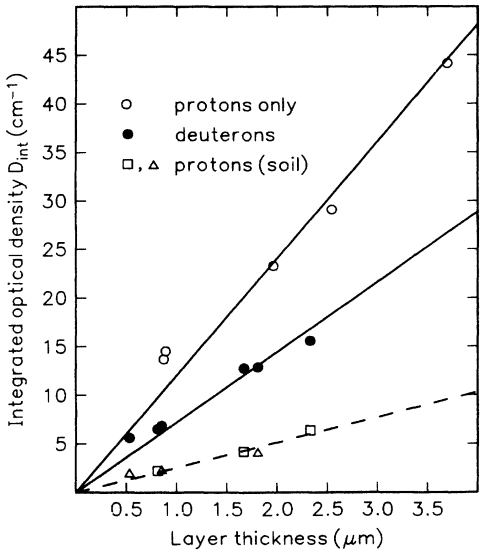

FIG. 3. The integrated optical density D_{int} of the proton- and deuteron-ir absorption bands for the fabricated waveguides, plotted against the layer thickness d_{50}. The dashed line accounts for residual proton content of the deuteron exchanged layers.

Thus, the absorption strengths per ion, $a_{H\text{-}D}$ can be calculated from the slope

$$\partial(D_{H\text{-}D})/\partial(d_{50}) = a_{H\text{-}D}c_{H\text{-}D}, \tag{7}$$

if the concentration of the protons and deuterons is known. The PE proton concentration is determined solely by the degree x of exchange according to

$$c_{H\text{-}D} = x_{H\text{-}D}[\mathrm{Li}], \tag{8}$$

assuming a replacement of Li by H, with [Li]= 1.885×10^{22} cm^{-3} for congruent $LiNbO_3$.

In this work, $x_{H\text{-}D}$ has not directly been measured, but with very reasonable arguments it can be fixed to the range $x = 0.70 \pm 0.05$: (i) Rice and Jackel (1984) found for $LiNbO_3$ powder that an increase of the buffering Li concentration in the melt from 0 to 3 mol% resulted in a linear decrease of x from 0.8 to 0.6.[11] We chose [Li] = 1.5 mol% in order to "tune" x to the central value 0.7. (ii) Richter *et al.* (1989) determined a depth resolved Li-concentration profile using SIMS and sputtering techniques for a waveguide fabricated under identical conditions compared to our samples. Because the abrupt increase of [Li] coincides with the sharp edge of the index profile, they deduced $x_H = 0.7$.[10] (iii) However, Canali *et al.* (1986) pointed out that analytic SIMS results are questionable because of matrix effects which strongly depend on the physicochemical properties being quite different for the exchanged layer and the bulk. Therefore, they used ion-bombardment-induced nuclear reactions with H and Li and monitored the resultant γ and α radiation, respectively. An exchange of 65–75% was observed for samples immersed in pure benzoic acid.[13]

In summarizing one can state that independent of the analytical method used, an exchange value around $x = 0.7$ is always found.

With the knowledge of x, the factor a_H is deduced from the upper straight line in Fig. 3 to be

$$a_H = (9.125 \pm 1.369) \times 10^{-18} \text{ cm}. \tag{9}$$

The experimental uncertainty of 15% originates mainly from the relative error in the value for x (8%), in the absolute scalings of the optical density (1.5%) and the layer thickness (1.5%) and the statistical variation in the data for all samples around the regression line (4%).

Despite all precautions taken in the fabrication process of the deuterated layers, traces of protons were found. Protons were introduced most likely during the handling of the deuterated benzoic acid.

The proton contribution can be determined and corrected for, assuming that the total degree of exchange of Li is written as the sum of the partial exchange rates $x_{total} = x_H + x_D$ and that $x_{total} = 0.7$ as for the purely proton-exchanged samples. The first assumption requires a homogeneous distribution of both species which is certainly fulfilled because of almost identical effective diffusion coefficients during the exchange process. We applied two procedures to separate the two contributions and to extract the absorption strength.

The first method assumes that the *ratio* $a_H/a_D = 1.88$ determined for rutile[9] is applicable to $LiNbO_3$. With the relation

$$\frac{D_H}{D_D} = \frac{a_H}{a_D}\frac{x_H}{x_D}$$

we calculated the values $x_H = 0.11$ and $x_D = x_{total} - x_H = 0.59$ from the observed ratio D_H/D_D. Using the slope of the deuteron optical density line in Fig. 3 and the value for x_D, we get $a_D = 6.5 \times 10^{-18}$ cm. The ratio of the rescaled quantities a_H and a_D turns out to be 1.40 and thus significantly smaller than the value of Johnson *et al.* for rutile.[9]

In contrast, the second method uses the proton traces to determine the ratio a_H/a_D. From Eqs. (1), (5), and (8) we derive the relation

$$\frac{D}{x} = a[\mathrm{Li}]d_{50} \tag{10}$$

for both protons and deuterons. In Fig. 4 we have plotted the quantity D/x versus the layer thickness d_{50} for the data points from Fig. 3. Because the slope a[Li] in Eq. (10) is independent of the rate of exchange, the fitted straight lines belonging to the data points of the pure PE layers and the proton traces from Fig. 3 must coincide in the presentation chosen in Fig. 4. From this condition we derive $x_H = 0.15$ for the proton traces and $x_D = 0.55$ in the deuteron exchanged layers. The ratio of the slopes in Fig. 4 yields the ratio

$$\frac{a_H}{a_D} = 1.31 \pm 0.10. \tag{11}$$

With the knowledge of the absolute value $a_H = (9.13 \pm 1.37) \times 10^{-18}$ cm determined from the purely proton-exchanged samples one arrives at

$$a_D = (6.96 \pm 1.60) \times 10^{-18} \text{ cm}. \tag{12}$$

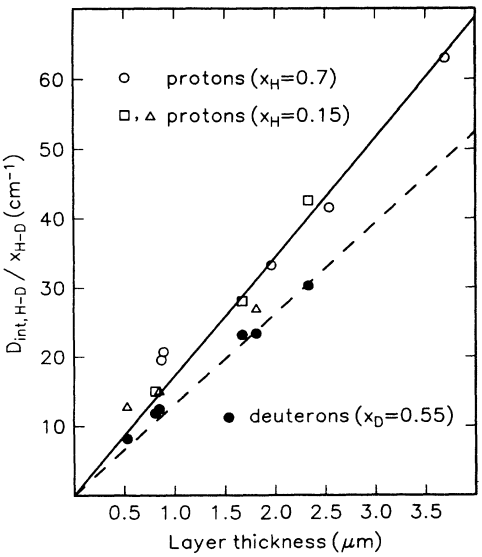

FIG. 4. The integrated optical density D_{int} normalized to the rate of exchange x of the proton- and deuteron-ir absorption bands for the fabricated waveguides, plotted against the layer thickness d_{50}. The absorption per ion values for protons and deuterons, a_H and a_D, respectively, are read from the slopes of the two linear fit lines.

Within the given accuracy this result agrees with that of the first method. We favor the second method, because it is only based on present experimental results and its self-consistent behavior.

B. Protonic dc conductivity

1. *Electric conductivity measurements*

Determination of the proton and deuteron content. The samples prepared for the electric dc measurements by annealing or field-enhanced in-diffusion showed the well-known broad OH-absorption band at 3485 cm^{-1} with its unresolved structure. The maximum of the corresponding OD band lies at 2569 cm^{-1}.[19] An annealing at 850 °C reduces the absorption constant to 0.22 cm^{-1}. Subsequent field-enhanced in-diffusion results in $\alpha_{\max}$ up to 12.5 cm^{-1}. Along with the raise of $\alpha_{\max}$ the bandwidth increases from 28 to 37 cm^{-1}. In addition, a change of the band shape is observed. The reproducibility and the mean experimental uncertainty in the determination of the integrated OH and OD optical density is less than 2%.

Using this doping procedure we were able to vary the proton concentration in the range 2×10^{17}–2×10^{19} cm^{-3}, while for deuterons the range was limited to somewhat more than 1 order of magnitude.

Determination of the electrical conductivity. For each sample prepared the electric conductivity σ for a given temperature T was calculated from the sample thickness d and electrode area A as an average over the currents I, measured for several external voltages U_{ext} applied, according to

$$j = \sigma E_{\text{ext}}, \quad j = \frac{I}{A}, \quad \text{and } E_{\text{ext}} = \frac{U_{\text{ext}}}{d}, \tag{13}$$

from the current density j and the driving electric field E_{ext}. No corrections for inhomogeneous field distributions were necessary because of the well-defined, thin-platelet geometry of the samples and the guard ring electrodes used. For each temperature and all proton concentrations, σ was found to be constant up to the highest electrical fields $E_{\text{ext}} = 2\times10^5$ V/cm achieved with thin polished samples. Thus no nonlinear effects, like high voltage break-throughs, up to electric fields comparable in strength to the inner electric fields have to be considered.

For all samples, the temperature dependence of σ showed an Arrhenius-like behavior. The same behavior was also found in diffusivity experiments. This suggests the validity of the Nernst-Einstein relation

$$\sigma = \frac{c e^2 D}{k_B T}, \tag{14}$$

which relates σ with the concentration c and charge e of the mobile species, the temperature T, and the diffusion constant D, which is expressed for a hopping process in the Arrhenius form

$$D = D_0 \exp\left(-\frac{\varepsilon_{act}}{k_B T}\right), \tag{15}$$

introducing the activation energy ε_{act} for the process. The pre-exponential factor D_0 of the diffusion constant contains the physical parameters of the microscopic jump process,

$$D_0 \approx \nu_a \bar{r}^2 \tag{16}$$

introducing the mean jumping distance $\bar{r}$ and the attempt frequency ν_a. Expressing the conductivity by

$$\sigma = \sigma_0 \exp\left(-\frac{\varepsilon_{act}}{k_B T}\right), \tag{17}$$

the pre-exponential σ_0 still depends on T according to

$$\sigma_0 = \frac{ce^2 D_0}{k_B T}. \tag{18}$$

In the semilogarithmic plot $\ln(\sigma T)$ versus the reciprocal temperature T^{-1}, the data for each sample falls on a straight line, the slope of which yields the activation energy (see Fig. 5). Within a scatter of 3.5% the activation energies obtained were equal for all samples of the pure, congruent $LiNbO_3$, either proton- or deuteron-doped: $\varepsilon_{\text{act,H}} = \varepsilon_{\text{act,D}} = 1.23 \pm 0.04$ eV. A slightly lower value was found for the two iron-doped samples: $\varepsilon_{\text{act,H,Fe}} = 1.17 \pm 0.01$ eV (see Fig. 6). In Table I the measured ir absorption, the scaled proton and deuteron concentration and the conductivity data are summarized for all samples prepared.

Our data for ε_{act} fit in the large range 1.0–1.5 eV of values reported in the literature.[20] Even for nominal pure $LiNbO_3$ samples such a large range has to be considered. In addition, doping crystals with different metal ions results in significant variations of ε_{act} depending on the

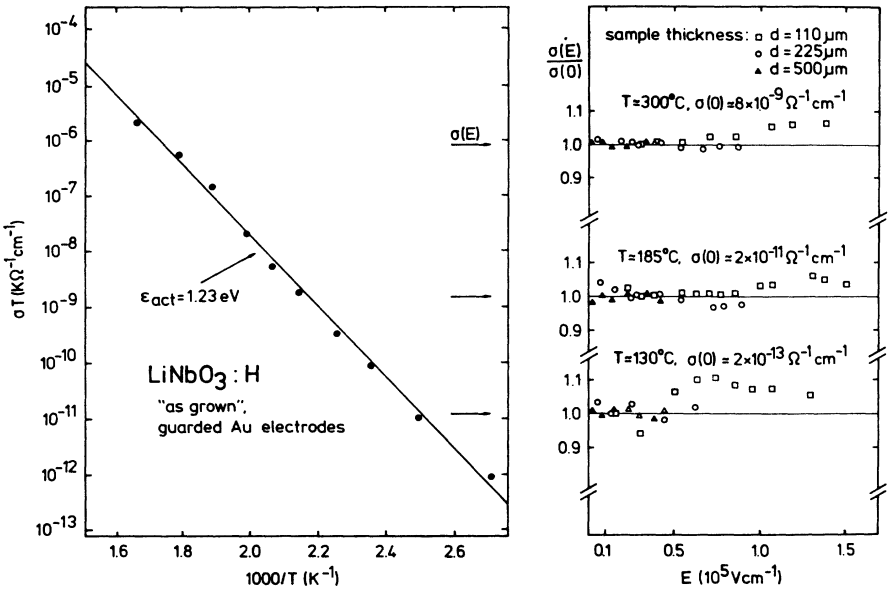

FIG. 5. Arrhenius plot $\ln(\sigma T)$ vs T^{-1} of the temperature dependence of the protonic conductivity σ in $LiNbO_3$ for the "as-grown" sample with an integrated ir absorption $A_{int} = 120\ cm^{-2}$ (left part). The three arrows point to conductivity values, where the dependence of σ from the applied electric field E was measured for thin polished samples (right part).

impurities added (Mg, Cu, Mo, W, Mn).[16]

An isotope effect in the activation energy might be due to the different quantum-mechanical zero-point energies of protons and deuterons vibrating in a binding potential. Taking the ir frequencies of the OH and OD modes $\hbar\omega_{H\text{-}D}$ of the OH and OD modes (2570 and 3485 cm^{-1}), the difference is expected to be $\frac{1}{2}(\hbar\omega_H - \hbar\omega_D) \approx 0.06$ eV. This is slightly above the variance of 0.04 eV given above.

The precise value of the activation energy is crucial for the determination of the pre-exponential factor. The quantity $\ln(\sigma_0 T)$ is obtained from an extrapolation of the straight line in the semilogarithmic plot from the range $T^{-1} \approx 1.2\text{–}2.6\times10^3\ K^{-1}$ to $T^{-1} = 0$. If the evaluation was restricted to only *one concentration value*, the consideration of the small 0.04-eV scatter for ε_{act} would yield already a variation of the absolute value of σ_0 by a factor of 2. Such a variation would not allow us to draw conclusive arguments for an isotope effect. To overcome this

TABLE I. Measured integrated ir absorption, used to determine the proton-deuteron concentrations, and extracted pre-exponential factors of dc conductivity for all samples prepared. The absorption is normalized to the case of polarized measurement.

ir absorption (cm^{-2})		Concentration (10^{18} cm^{-3})		Pre-exponential (10^4 K/Ωcm)	
$(A_{int})_H$	$(A_{int})_D$	c_H	c_D	$(\sigma_0 T)_H$	$(\sigma_0 T)_D$
		Proton-doped samples, 660 ppm Fe ($\varepsilon_{act} = 1.17 \pm 0.02$ eV)			
29.6		1.41		0.58 ± 0.03	
326.6		15.56		6.49 ± 0.21	
		Proton-doped samples ($\varepsilon_{act} = 1.23 \pm 0.04$ eV)			
15.5		0.73		1.01 ± 0.07	
44.0		2.08		1.76 ± 0.12	
119.8	(as grown)	5.65		3.86 ± 0.45	
184.8		8.72		3.04 ± 0.24	
597.2		28.23		14.74 ± 1.35	
912.4		43.05		22.48 ± 1.57	
		Deuteron-doped samples ($\varepsilon_{act} = 1.23 \pm 0.04$ eV)			
16.6	218.1	0.79	13.62		5.16 ± 0.33
107.6	488.3	5.12	30.51		11.82 ± 0.92
41.9	816.1	1.99	50.98		19.75 ± 0.63

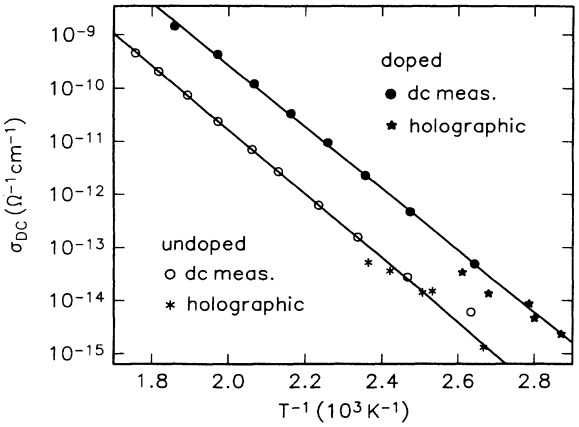

FIG. 6. Comparison of the directly and holographically measured dc conductivity of the iron-doped $LiNbO_3$ sample. The lines were fitted to the directly measured dc data, i.e., • and o for the proton-doped and the undoped "as-grown" sample, respectively, ⋆ and * refer to the holographic data of the proton-doped and undoped sample, respectively.

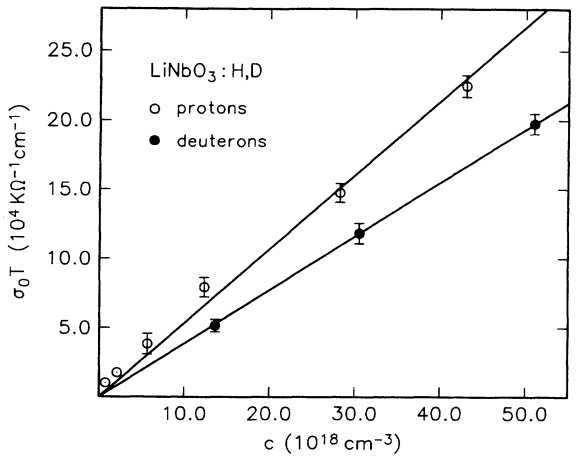

FIG. 8. The pre-exponential quantity $\sigma_0 T$ for the proton and deuteron samples plotted against the charge carrier concentration c, scaled from the integrated ir absorption intensity A_{int}, using the absorption per ion values $a_{H\text{-}D}$ determined in this paper.

difficulty we took advantage of our measured concentration dependence, see Fig. 7.

Using the same activation energy in the extrapolation for all samples, the linear correlation over 2 orders of magnitude between the electrical conductivity in the temperature range investigated and the proton and deuteron concentration calibrated from the ir absorption is preserved also in the pre-exponential σ_0.

In Fig. 8 the quantities $\sigma_0 T$ are plotted in a linear-linear manner versus the charge carrier concentration c. Two well-separated straight lines result for protons and deuterons, reflecting the linear relation $(\sigma_0 T) \sim c$ implied by Eq. (18). The difference in their slopes,

$$R_{H\text{-}D} \equiv \frac{\partial(\sigma_{0,H\text{-}D}T)}{\partial(c)}$$

is due to the isotope effect which, according to the hopping model implied in Eq. (16), results from the mass dependent difference in the attempt frequencies

$$\nu_a \sim \mu^{-1/2}. \tag{19}$$

Here, μ is the reduced mass of the vibrating bound ion attempting to hop.

For the case of a proton or a deuteron bound by an oxygen the frequency ratio will become $f_H/f_D = (\mu_{OD}/\mu_{OH})^{1/2} = 1.374$, which is slightly below the value $(m_D/m_H)^{1/2} = 1.414$ for the protons and deuterons bound to infinite mass. In contrast to this, mobile hydroxyl ions (OH^- or OD^-) would yield $f_{OH}/f_{OD} = (18/17)^{1/2} = 1.029$. Such a small difference could hardly be distinguished. From Fig. 8 we read for the *ratio* of the slopes of the two straight lines fitting the experimental data $R_H/R_D = 1.36 \pm 0.17$, which is in perfect agreement with the model of hopping protons and deuterons.

The *absolute* value of R_H is needed to extract the pre-exponential diffusion constant and the physical parameters contained therein. It depends on the value of the calibration factors $a_{H\text{-}D}$. We yield

$$R_H = (5.3 \pm 1.1) \times 10^{-15} \frac{\text{K cm}^2}{\Omega}$$

and

$$R_D = (3.9 \pm 0.8) \times 10^{-15} \frac{\text{K cm}^2}{\Omega}.$$

Here, the errors account for the absolute scalings of the factors $a_{H\text{-}D}$, the electrode areas, sample thickness, and the accuracy of the electrometer. But we should mention, that small variations of the activation energy and their

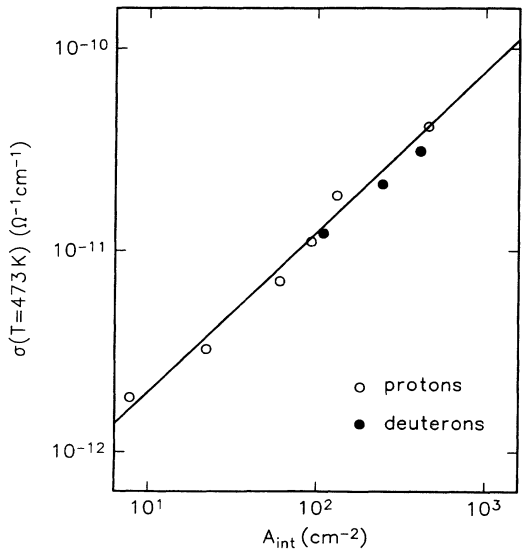

FIG. 7. The protonic conductivity σ at 200 °C (473 K) of the proton and deuteron doped samples as a function of the integrated ir OH and OD absorption band intensity A_{int} near 3485/2570 cm^{-1}, respectively.

influence on the absolute values of the pre-exponentials $R_{H\text{-}D}$ is not contained in these error bars.

The quantities R_H and R_D together with the activation energy ε_{act} and the gauge factors a_H and a_D summarize all our data on the protonic conductivity. Their knowledge allows to predict by means of Eqs. (1), (17), and (18) the dark conductivity for pure congruent $LiNbO_3$ from a simple measurement of the integrated OH and OD absorption.

2. *Holographic conductivity measurements*

The concept of this method is to monitor the decay in the diffraction efficiency of volume phase holograms. The experimental procedure was sketched above and the theory for data evaluation is summarized as follows. The diffraction efficiency η of a grating is defined as the ratio $\eta = I_d/(I_t + I_d)$, from the intensities of the diffracted and the transmitted beams, I_d and I_t, respectively. The quantity η is expressed in terms of the parameters of the grating and beam geometry using the Kogelnik equation[21]

$$\eta = \left(\sin \frac{\pi \Delta n\, g}{\lambda_e \cos\theta_i}\right)^2, \tag{20}$$

which involves the wavelength λ_e of the laser beam outside the crystal, the angle of incidence θ_i of the two beams symmetric to the surface normal, the grating period g, and the total modulation Δn of the refractive index caused by the periodic space-charge pattern. When the charges become mobile the modulation relaxes with time according to $\Delta n(t) = \Delta n(0)\exp(-t/\tau)$, where the relaxation time τ is related to the electrical conductivity σ via[22]

$$\tau = \frac{\varepsilon_0 \varepsilon}{\sigma}. \tag{21}$$

The relevant dielectric constant ε_z for $LiNbO_3$ is taken to be $\varepsilon_z = 28.5$ from Ref. 23. The Kogelnik equation (20) yields

$$\Delta n(t) \sim \arcsin[\sqrt{\eta(t)}],$$

which allows to extract the desired time constant τ. The results are summarized in Fig. 6, where we plotted the conductivity data from the direct electrical dc measurements together with the fitted Arrhenius dependence ($\varepsilon_{act} = 1.17$ eV) for the H-doped and the undoped $LiNbO_3$:Fe samples. The holographically measured data fall on the extrapolation of the Arrhenius lines. The increase in proton content by a factor of 10 is perfectly reflected in the increase of conductivity, measured with both methods, see Fig. 5. For temperatures close to 140 °C, the holographic values slightly deviate below the fitted lines as a consequence of the very rapid decay of the holograms. This limited the range of application of the holographic method at still higher temperatures.

IV. DISCUSSION OF RESULTS

A. Determination of the concentration-calibration factors

The knowledge of the concentration of the mobile charges in a crystal is necessary to extract the physical parameters (e.g., the diffusion constant and the parameters therein) and the isotope effect of the process of mi-

TABLE II. Comparison of the calibration factors for the proton and deuteron concentration, scaled from the OH-OD stretch mode absorption in different oxidic crystals.

Material	Cross section (10^{-20}cm^2)	Position (cm^{-1})	Γ cm^{-1}	a_H 10^{-19}cm	Calibration method	Ref.
$LiNbO_3$ (PE)	41.5	3508	44	91 ± 14 Protons	PE layers, degree of exchange known	This work
		2593	29	70 ± 16 Deuterons		
$LiNbO_3$ (PE)	40 ± 20	3508	45 ± 6	89 ± 55	PE layers, degree of exchange known	10
TiO_2	230	3276	20[b]	251 ± 9[a] Protons	Change of mass due to doping	[a] 9
		2437	8[b]	133 ± 5[a] Deuterons		[b] 29
$LiNbO_3$	3.3 ± 1.1	3485	30	6.8 ± 2.3	NMR	24
$LiNbO_3$:Mg,M	6 ± 3.8	3522 3506	10	4.1 ± 2.3	ir absorption of Mg-OH-M associates	8
$KTaO_3$:Fe	23 ± 11	3472	4	6.6	EPR of Fe^{3+} associated to H^+	25

gration from conductivity measurements. This is evident from the basic Nernst-Einstein relation [Eq. (14)].

In the literature much work is found on calibration factors which allow us to calculate the proton concentration in different oxidic crystals from the intensity of the absorption band of the O↔H stretching vibration. Unfortunately, most authors simply take the absorption constant α_{max} at the maximum of the OH band as the relevant measure of intensity,[24,25,10,26] and calculate the cross section for the absorption process according to $w = \alpha_{max}/c$. Because the shape of the OH- and OD-absorption spectra depends on the material, its composition and the isotope, the quantity α_{max} alone is not useful for comparisons. In Table II we present a comparison of the data for different oxidic materials obtained with several methods to determine the concentration $c_{H\text{-}D}$, from the cross section w, typical half-widths Γ, and the $a_{H\text{-}D}$ factors. From these data it is clear, that the absorption per ion, $a_{H\text{-}D}$, is the adequate quantity to compare. For example, the bandwidth Γ for the OH mode varies between 4 cm^{-1} for pure $KTaO_3$, about 30 cm^{-1} for congruent $LiNbO_3$ and up to 44 cm^{-1} for proton-exchanged $LiNbO_3$.

The a_H factors of Table II have been calculated from the cross sections w given in the literature using the approximate form $A_{int} \approx \mathcal{F}\alpha_{max}\Gamma$, where Γ is defined as the full width at half maximum of the peak (FWHM) and $\mathcal{F}$ is a form factor accounting for the peak form. Assuming Lorentzian-shaped peaks, i.e., using $\mathcal{F} = \pi/2 = 1.57$, one approximates A_{int} to 10% accuracy.[9] This was used in Table II except for the absorption bands of proton-exchanged layers, where $\mathcal{F} = 1.15$ was found as a good approximation.

Comparing the different values for the absorption per ion a_H one finds variations over nearly 2 orders of magnitude. Probably the most direct method is that of Johnson *et al.* for TiO_2,[9] where the changes in the mass of the samples due to successive exchange of protons and deuterons obtained by annealing the samples in humid atmosphere were measured. In all the other works cited, the cross section w was determined by merely indirect methods: Bollmann *et al.*[24] compared the intensities of the proton resonance signals in doped $LiNbO_3$ crystals with those of various other substances of which the protons are part of the chemical composition. Thus the resultant proton resonance signal had to be extrapolated over 2 orders of magnitude down to the low proton concentrations in the H-doped $LiNbO_3$ crystals. Kovàcs *et al.*[26] attribute new bands appearing in $LiNbO_3$:Mg:*M* for M = Nd,Cr to M-OH-Mg complexes and scale the H concentration with the values of the dopant concentration [M] in the melt during crystal growth. Lee *et al.*[25] scaled the value of w in a similar way via the intensity of an Fe associated OH band in $KTaO_3$. Finally, Richter *et al.*[10] also investigated proton exchanged layers in $LiNbO_3$. Using their results to calculate a_H yields very good agreement with the result of the present work. We point out that the measurements performed on proton-exchanged layers yielded the largest values for w in $LiNbO_3$. The experimental uncertainty for the a_H values scaled from proton-exchanged data is governed by the uncertainty in the degree of exchange. Even the largest possible scatter, i.e., $x_H = 0.7 \pm 0.3$ cannot account for the large variations reported in the literature. But due to Rice and Jackel,[11] the value for $x_H \approx 0.7$ is limited to 0.6–0.8 for low Li concentrations in the melt. Therefore we believe that the data obtained for PE layers are the most accurate for $LiNbO_3$.

The question, whether the absorption cross sections deduced from bulk and PE layers are comparable, needs to be discussed, too. For proton-exchanged layers in $LiNbO_3$ the absorption constant reaches values $\alpha_{max,\,PE} = (5\text{–}9)\times 10^3$ cm^{-1}, which must be compared to bulk values of the order $\alpha_{max,bulk} = 1\text{–}10$ cm^{-1}. Therefore the proton concentration in PE layers are larger by 3 orders of magnitude. Additionally, due to the one-to-one exchange the Li concentration in the layers is reduced to about 30% compared to the bulk. In view of the expected changes in the crystal structure it seems noteworthy here to recall some facts concerning the OH-vibration band: Both the OH- and the OD-vibration band in layers were found to be polarized perpendicular to the c axis of the crystals as it is the case in the bulk band. The bulk polarization was already interpreted by Herrington *et al.*[27] to be due to protons vibrating along the nearest O–O distances which occur in the typical oxygen triangles of the $LiNbO_3$ structure. The small frequency shift of about 70 cm^{-1} from the nominal value of the free OH^- ion[28] and the identical polarization behavior of the bulk and the PE band lead to the assumption, that the protons in PE layers also form ir-active OH dipoles which are rather weakly influenced by the other changes of the physicochemical properties of the exchanged layers. The exchanged protons obviously do not occupy Li sites but again attach an oxygen and orient along the nearest O–O bonds.[12] From these arguments it seems reasonable to use the calibration factors $a_{H\text{-}D}$ obtained for proton exchanged layers also to determine the proton and deuteron concentration of the bulk.

Beside the absolute a_H values obtained in this work, the isotope effect for the proton and deuteron band intensities, which manifests in the ratio a_H-a_D, is crucial for the determination of the isotope effect in the electrical conductivity. As outlined in detail in the paper of Bates and Perkins,[29] the ratio of the absorption band intensities per ion for absorbing modes which only differ in an isotopic change of the ions 1 (=H) and 2 (=D) participating in the excited mode is given in the harmonic approximation by

$$\frac{a_1}{a_2} = \left[\left(\frac{\bar{\nu}_1}{\omega_{e,1}}\right) \Big/ \left(\frac{\bar{\nu}_2}{\omega_{e,2}}\right)\right] \times \left[\left(\frac{dp_1}{dQ_1}\right)^2_{Q_{e,1}} \Big/ \left(\frac{dp_2}{dQ_2}\right)^2_{Q_{e,2}}\right], \tag{22}$$

where

$$\left(\frac{dp}{dQ}\right)_{Q_e} = \mu^{-1/2}\left(\frac{dp}{dr}\right)_{r_e}.$$

Here $\bar{\nu}$ denote the spectral frequency positions of the bands, ω_e are the spectroscopic parameters appearing in the term value formula for a diatomic anharmonic oscilla-

tor established by Herzberg.[30] The normal coordinate Q is defined from the interatomic displacement coordinate $\Delta r = (r - r_e)$ by $Q = \mu^{1/2}\Delta r$, where μ is the reduced mass of the two-atomic system with its equilibrium positions r_e or Q_e. The ratio a_1/a_2 is related to the ratio of the oscillator strengths f:

$$\frac{a_1}{a_2} = \frac{\mu_2}{\mu_1}\frac{f_1}{f_2}. \tag{23}$$

The spectroscopic parameters ω_e can be deduced from anharmonic frequency shifts seen, e.g., in overtone spectroscopy. Values for ω_e for the band in proton- and deuteron-exchanged layers have been determined experimentally: $\omega_{e,H} = 3674 \pm 10$ and $\omega_{e,D} = 2686 \pm 10$ cm^{-1}.[19] Using the band frequencies $\bar{\nu}_H = 3508$ cm^{-1} and $\bar{\nu}_D = 2593$ cm^{-1} the first factor in Eq. (22) is almost equal to unity, i.e., 1.02. The same occurs also in TiO_2.[29]

Wedding and Klein[31] obtained $f_1/f_2 = 2.52 > 1$ for the alkali halides using the dependence of the first electric moment p on the O–H distance calculated by Cade.[32] Bates and Perkins[29] worked out the theoretical background to the experimental results of Johnson *et al.*,[9] where for TiO_2 it was found that $a_H/a_D \approx \mu_D/\mu_H = 1.88$. This yields $f_H/f_D \approx 1$, which is considerably smaller compared to the alkali halides. Within 2% the relation $a_1/a_2 = \mu_2/\mu_1$ was fulfilled for all three isotopes H, D, and T in TiO_2.[29] This shows that in TiO_2 the dipole derivative dP/dr depends only slightly on the mass. Our value $a_H/a_D = 1.31 \pm 0.10$ for OH and OD in $LiNbO_3$ means that $f_H/f_D \approx 0.69 < 1$ which is even considerably smaller than in TiO_2. This difference of more than 30% is too large to be caused by an inappropriate treatment of the degree of exchange of the deuterons which was the main contribution to the experimental uncertainty (see Sec. III A). Therefore we conclude, that within the harmonic approximation the dipole derivative may well become mass dependent. Unfortunately, no data are available for this quantity in $LiNbO_3$.

Obviously the situation for OH and OD in oxidic crystals may not be compared to the behavior of these defects in the alkali halides. In oxidic materials the oxygen atom is part of the crystal lattice, which determines its electronic structure. In the alkali halides, OH^- is a substitutional defect which may behave more like the unperturbed OH^- ions, for which theoretical calculations are less complicated.

This difference is even more pronounced when the absolute values of the oscillator strength f_H are compared. We used the Smakula equation

$$c_H f_H = \frac{A_{int}\mu c_0^2}{\pi e^2}\frac{9n}{(n^2+2)^2} \tag{24}$$

to calculate f_H from the absorption per ion $a_H = A_{int}/[c_H \cdot \ln(10)]$. Here, $e = 4.803 \times 10^{-10}$ esu is the elementary charge, c_0 the velocity of light, n the refractive index at the absorption wavelength, and μ the reduced mass.

Using the calibration value a_H obtained in this work yields $f_H = 1.7 \times 10^{-2}$ for $LiNbO_3$. The data of Johnson *et al.* yield $f_H = 3.8 \times 10^{-2}$ for TiO_2, which is close to the $LiNbO_3$ value. By comparison, using the same form of the Smakula equation, f_H values in the alkali halides fall into the range (5×10^{-4})–(5×10^{-3}),[31] which is roughly an order of magnitude below the values for oxidic crystals.

Finally we want to comment on the method of scaling the proton concentration from ir absorption. Richter *et al.*[10] reported that the OH band was restored at the bulk position with practically the same maximum absorption and half-width when the waveguides were annealed at 350 °C for, e.g., 10 h. This was attributed to an unchanged cross section. But this conclusion only holds if the total proton content remained constant. The latter has to be checked because of the following experimental findings: The integrated absorption A_{int} shows a striking hysteresis feature. When heating samples up to $\approx$ 300 °C, A_{int} decreases and does not return immediately to the original value, when cooled down. The delay depends on the sample and can last several hours.[33]

B. Protonic conductivity and ir absorption

We start this section with a comparison of the measured protonic conductivity values and the various results for the conductivity given in the literature, summarized by Kovàcs and Polgar.[20] At T = 400 °C an "as grown" sample yields a conductivity of $\sigma = 2.9 \times 10^{-6}(\Omega\,m)^{-1}$ using the data given in Table I and Eqs. (17) and (18). This falls into the narrow range 10^{-6}–$10^{-5}(\Omega\,m)^{-1}$ of all known literature data.[20] The variation of data is probably simply due to different "as-grown" proton concentrations. An extrapolation of our data to $RT = 20$ °C would yield $8.3 \times 10^{-18}(\Omega\,m)^{-1}$ which is about ten times below the value $10^{-16}(\Omega\,m)^{-1}$ estimated from the decay of holograms by Staebler and Amodei.[2] This is consistent with the findings of other authors who measured with indirect methods that the activation energy drastically decreases below 0.5 eV somewhere in the range $T = 60$–100 °C (see the summary in Ref. 20). For example, Blistanov *et al.*[16] found $\varepsilon_{act} = 0.49$ eV for $T < 80$ °C. The abrupt change in ε_{act} indicates that another mechanism dominates at these temperatures, probably electron or (small) polaron hopping, so that an extrapolation is principally not appropriate.

Furthermore we discuss the good agreement of the conductivity data obtained with the direct electrical dc and the holographical method, and the perfect correlation with the increase in bulk proton content measured subsequently with the same samples. This agreement indicates three facts: First, surface currents in direct dc measurements have succesfully been eliminated by the use of guard electrodes. This probably cannot trivially be assured from direct current measurements alone. Blistanov *et al.* report on a determination of the separated contributions of bulk and surface conductivity σ_b and σ_s, respectively, using indirect methods. They found that σ_s values were comparable with those of σ_b for temperatures below 200 °C and furthermore that the temperature dependence of σ_s for a pure crystal was even identical to that of σ_b.[16] We have confirmed this result when the guard electrodes were eliminated. Second, for the holo-

graphic read-out at low laser power, the contribution of photoconductivity can be neglected compared to the protonic one. The mobility of the protons then completely governs the relaxation process. Third that the absolute scaling of the direct dc values is in very good agreement with the scaling of the holographic method, thus assuring their reliability.

A detailed model on the microscopic migration process is not yet established. Some authors try to relate the physical parameters of the proton migration process, see Eq. (16), simply to the properties of the ir-absorption band.[8] But clear arguments are outlined below that the microscopic process is still not fully understood.

Let us now consider the meaning of the activation energy ε_{act} entering the simple hopping model described by the Arrhenius equation for the diffusion coefficient and the Nernst-Einstein relation to electric conductivity. In a classical picture ε_{act} is the energetic difference between the energy of the migrating species in the bound ground state of the system and the energy of the saddle-point configuration, i.e., when the migrating particle is midway between its two bound positions. The validity of the Nernst-Einstein relation for the migration of protons in the temperature range 100 to more than 700 °C is assured by the equality of the values measured for ε_{act} in diffusion experiments, e.g., $\varepsilon_{act} = 1.4$ eV,[34] 1.1 eV,[8] and conductivity measurements. The proton is believed to jump to the nearest O^{2-} ion from its previous bound position close to an oxygen. The binding potential for these hydroxyl complexes is usually described by a Morse-type potential and the potential parameters could be derived from ir-spectroscopic overtone data. In $LiNbO_3$ a value for the dissociation energy of 4.2 eV was determined.[19] This value represents the energy to break the bond completely. It is much higher than the activation energy for a jump in the migration process determined from the conductivity data. We should mention that an energetic barrier as low as ε_{act} can be constructed by simple superposition of two equivalent Morse-potentials "back to back," the second one fixed to the target oxygen ion of the jumping process. When two such potentials are pushed to each other as close as required by the O–O distance (about 280 pm), the remaining barrier in between actually decreases to values close to ε_{act}. But this is accompanied by the fact that the curvatures in the two minima of the sum potential are drastically lowered resulting in a significant decrease of the vibrational frequency. Such models have been discussed in connection with the frequency lowering of the OH mode in $LiNbO_3$ when the O–O distances were shortened due to high hydrostatic pressure up to 16 GPa applied to the crystal.[35]

On the other hand even the zero-pressure configuration of such constructed double-well potentials already exhibit strong anharmonicities, which contrast to the rather harmonic behavior actually found for the first overtone (i.e., the $v = 0 \rightarrow 2$ transition).[19] The state $v = 3$, which was observed recently in second overtone excitation ($v = 0 \rightarrow 3$) for heavily proton exchanged layers at 9989 ± 10 cm^{-1} or ≈ 1.2 eV,[36] would even lie above the barrier. These arguments demonstrate that the potentials and energy levels of the OH oscillator observed in ir spectroscopy do not agree with the low activation energy found in protonic conductivity and diffusion. The influence of the complex electronic charge distribution of the vibrating OH oscillator, its polarizing influence on the nearest ions must certainly be accounted for.

A detailed theoretical calculation for the diffusion of protons in TiO_2 did resolve a similar case and brought microscopic insight into the process.[37] Similar to trigonal $LiNbO_3$, the OH band in TiO_2 is polarized perpendicular to the tetragonal axis. From careful studies of the spectroscopic properties of the three isotopes protons, deuterons, and tritons the dissociation energy of the Morse potential used to describe the vibrational term values was found to be 2.7 eV (Ref. 29) whereas the experimental activation energies for the diffusion of protons were found to be different for directions parallel and perpendicular to the tetragonal axis, $\varepsilon_{act,\parallel} = 0.59$ and $\varepsilon_{act,\perp} = 1.28$ eV. The precise path of diffusion from one site to another could be calculated and the energy values were reproduced as the difference of the minimum saddle-point energy of the configuration for various paths and the ground state of the proton bound to an oxygen. The following contributions to the potential were taken into account: the electron density distribution of the hydroxyl ion to determine the equilibrium positions calculated from the wave function, a Morse potential to represent the O–H bond, the interaction of the charged proton with the induced electric dipole moments on the nearest O^{2-} ions, the Coulomb interaction with the charges of the neighboring Ti cations, and finally a repulsive short-range interaction of the hydroxyl with the Ti ions. The polarization of the OH vibration perpendicular to the c axis is strikingly reflected in the pre-exponentials diffusion constants: The value $D_{0,\perp} = 3.8 \times 10^{-1}$ cm^2/s is more than 2 orders of magnitude higher than $D_{0,\parallel} = 1.8 \times 10^{-3}$ cm^2/s.[37] For an interpretation of the corresponding attempt frequencies $\nu_{a,\perp}$ and $\nu_{a,\parallel}$, Bates *et al.*[37] assumed a superposition of the two librational modes $\omega_\perp$ and $\omega_\parallel$ of the OH oscillator, i.e., $\nu_{a,\perp} = 2\omega_\parallel + \omega_\perp$ and $\nu_{a,\parallel} = 2\omega_\parallel$. In $LiNbO_3$ both, the activation energy and the pre-exponential factors of the diffusion, e.g.,[34] and the electrical conductivity, e.g.,[20] and references therein, were found to be isotropic. Therefore an application of the model is not straightforward. In order to get a similar insight for $LiNbO_3$ a comparable model calculation is asked for, but so far beyond the scope of this work.

Let us further consider the values for pre-exponential factor. Kovàcs *et al.* measured a pre-exponential diffusion constant $D_{0,H} \approx 0.1$ cm^2/s and obtained rough agreement with Eq. (16). They choose a jumping distance of 300 pm as the O–O bond length in $LiNbO_3$ and an attempt frequency equal to the OH stretch-mode frequency to yield $D_0 = 0.16$ cm^2/s.[8] Other authors report even smaller values for D_0, 0.035, or 0.057 cm^2/s. The two different values were attributed to OH^- on interstitial or O^{2-} sites.[4] Bollmann[5] compares these low values even with the effective diffusion constant of the exchange front in the formation of proton exchanged layers, 0.087 cm^2/s (Ref. 5) or ≈ 0.01 cm^2/s.[13] The values for D_0 extracted from the pre-exponential σ_0 obtained in this work

according to Eq. (18) is 2.84 cm^2/s. Even the use of the lowest of the values a_H summarized in Table II yields $D_0 = 0.21$ cm^2/s, which is still more than a factor of 2 above the directly measured D_0 values.

Although the details of the microscopic process are still unclear, the results of this work have at least uniquely revealed the nature of the migrating species in $LiNbO_3$. The linear relation of the electric conductivity with the absorption constant for the OH vibration has so far not been proven before over more than 2 orders of magnitude. While some authors ascribe the migration to protons,[3] others repeatedly invoked hydroxyl ions.[4,5] Even though the positive sign of the effective charge could be concluded from spatially resolved ir absorption of a holographic pattern[3] or the profile obtained after field enhanced in-diffusion,[1,38] this does not allow us to distinguish between protons or hydroxyls. Migrating hydroxyls (OH^-) on the site of an oxygen (O^{2-}) also represent effectively positive charges with respect to the unperturbed lattice, as Bollmann pointed out.[5]

The decision is possible with a precise determination of the isotope effect in the pre-exponential factor when replacing protons by deuterons or tritons. Several works on the diffusion of all three isotopes have already been published,[7,34,8] but the experimental uncertainty for D_0 was too large to draw firm conclusions. In principle, diffusion experiments are to be preferred to conductivity measurements in view of a determination of the attempt frequency and jumping distance parameters of the migration process. According to Eq. (16), no other quantities are involved in D_0. An evaluation of the pre-exponential σ_0 always involves the crucial determination of the concentration of the charge carriers, see Eq. (14).

Despite the fact that the concentration dependence of σ_0 is usually a drawback of conductivity experiments compared to diffusion experiments,[39] it is just the linear concentration dependence of $\sigma_{0,\mathrm{H\text{-}D}}$ experimentally explored in this work, see Figs. 7 and 8, that yields an uncertainty for R_H/R_D as low as 13%.

Finally we mention that we obtained the ratio $R_H/R_D = 1.36$, which is in surprisingly perfect agreement with the value $(\mu_{OD}/\mu_{OH})^{1/2} = 1.374$ expected for protonic migration, according to Eq. (19). This R_H/R_D value reflects the use of the a_H/a_D ratio determined in this work. Larger a_H/a_D values were found for OH and OD in TiO_2 or the alkali halides. These values would result in a larger isotope effect of the conductivity, when applied here.

V. SUMMARY AND CONCLUSION

The aim of the present work was to bring insight into the migration of protons in $LiNbO_3$ in the temperature range 100–600 °C by means of direct dc measurements of the electric conductivity.

The migration was very early ascribed to the presence of protons in the crystals monitored by the absorption band at 3485 cm^{-1} of the O–H stretching vibration. The final decision on the nature of the migrating species, either protons or hydroxyl ions, could not be established. Neither the linear relation of the electric conductivity with the strength A_{int} of the OH absorption, which is reported in this work over the range of 2 orders of magnitude, nor the known positive sign of the effectively positive migrating charge[3] can be used to draw a final conclusion. An OH^- ion at the site of an O^{2-} also represents an effectively positive charge with respect to the unperturbed lattice.[5]

Together with the dc measurements, the absorption per ion for the ir absorption of the OH-stretch mode at about 3500 cm^{-1} was determined. For this purpose we used the absorption spectra of proton and deuteron exchanged layers, for which the proton concentration is known from the rate of exchange $x_H = 0.7$. The absorption per OH ion is one third of that in TiO_2, but still more than an order of magnitude higher than values estimated in other studies. Because these absorption strength factors are necessary to determine the concentration of the charge carriers in the migration process, arguments are given in favor of our calibration.

The isotope effect in the pre-exponential factor σ_0 of the electric conductivity of protons and deuterons has been measured. The ratio $(\partial\sigma_0 T/\partial c)_H/(\partial\sigma_0 T/\partial c)_D$ was found to be 1.36. This is in perfect agreement with the ratio $(\mu_{OD}/\mu_{OH})^{1/2} = 1.374$ expected in a simple hopping model from the relation $f_a \sim m^{-1/2}$ for the attempt frequency. Such a large isotope effect unequivocally proves that the protons are the migrating species rather than hydroxyls. The precise value depends on the calibration of the proton and deuteron concentration. The use of larger f_H/f_D ratios for the oscillator strength as found in TiO_2 or the alkali halides would yield a more pronounced isotope effect in the conductivity.

A holographic method was also used for reference to measure the protonic conductivity. The method does not suffer from the problems of short-cut surface currents and electrode contacts. It complements in an ideal manner the direct dc measurements because the temperature range could be explored down to 80 °C. The results of both methods perfectly agree with each other with respect to the temperature, the concentration, and the electric field dependence of the protonic conductivity. The electric conductivity was found to be independent of the electric field, checked up to values comparable to the strength of inner electric fields. These results show that the migration of the protons influences the temperature stability of holograms via the dark conductivity.

The microscopic mechanism of the migration is still unclear. We believe that more sophisticated theoretical models like those for TiO_2 (Ref. 37) are necessary for $LiNbO_3$ too, in order to give insight into the microscopic process of migration.

ACKNOWLEDGMENTS

This work was supported by the Deutsche Forschungsgemeinschaft, SFB 225 (Oxidic crystals for electro- and magnetooptical applications)/C1. Dr. R. Sommerfeldt is gratefully acknowledged for valuable help during the holographic and the mode-coupling experiments.

[1] R. G. Smith, D. B. Fraser, R. T. Denton, and T. C. Rich, J. Appl. Phys. **39**, 4600 (1968).
[2] J. J. Amodei and D. L. Staebler, Appl. Phys. Lett. **18**, 540 (1971).
[3] H. Vormann, G. Weber, S. Kapphan, and E. Krätzig, Solid State Commun. **40**, 543 (1981).
[4] W. Bollmann and H. J. Stöhr, Phys. Status Solidi A **39**, 477 (1977).
[5] W. Bollmann, Phys. Status Solidi A **104**, 643 (1987).
[6] J. L. Jackel, C. E. Rice, and J. J. Veselka, Appl. Phys. Lett. **41**, 607 (1982).
[7] R. Gonzalez, C. Ballestros, Y. Chen, and M. M. Abraham, Phys. Rev. B **39**, 11 085 (1989).
[8] L. Kovàcs, K. Polgar, R. Capelletti, and C. Mora, Phys. Status Solidi A **120**, 97 (1990).
[9] O. W. Johnson, J. DeFord, and J. W. Shaner, J. Appl. Phys. **44**, 3008 (1973).
[10] R. Richter, T. Bremer, P. Hertel, and E. Krätzig, Phys. Status Solidi A **114**, 765 (1989).
[11] C. E. Rice and J. L. Jackel, Mater. Res. Bull. **199**, 591 (1984).
[12] M. Rottschalk, Dissertation, University of Jena, German Democratic Republic (1988).
[13] C. Canali, A. Carnera, G. DellaMea, P. Mazzoldi, S. M. Al-Shukri, A. C. G. Nutt, and R. M. DeLaRue, J. Appl. Phys. **59**, 2643 (1986).
[14] P. K. Tien, R. Ulrich, and R. J. Martin, Appl. Phys. Lett. **14**, 291 (1969).
[15] P. Hertel and H. P. Mentzler, Appl. Phys. B **44**, 75 (1987).
[16] A. A. Blistanov, E. V. Makarevskaya, V. V. Geras'kin, O. Kamalov, and M. M. Koblova, Fiz. Tverd. Tela (Leningrad) **20**, 2575 (1978) [Sov. Phys. Solid State **20**, 1489 (1978)].
[17] A. A. Blistanov, V. V. Geras'kin, A. V. Stepanova, M. V. Puchkova, and N. G. Sorokin, Fiz. Tverd. Tela (Leningrad) **26**, 1128 (1984) [Sov. Phys. Solid State **26**, 684 (1984)].
[18] R. Sommerfeldt, Dissertation, University of Osnabrück, Federal Republic of Germany, 1989.
[19] A. Förster, S. Kapphan, and M. Wöhlecke, Phys. Status Solidi B **143**, 755 (1987).
[20] L. Kovàcs and K. Polgar, in Properties of Lithium Niobate (EMIS Datareview Series No. 5, 1989), RN=16037, p. 109.
[21] H. Kogelnik, Bell Syst. Techn. J. **48**, 2909 (1969).
[22] T. J. Hall, R. Jauna, L. M. Connors, and P. D. Foote, Prog. Quantum Electron. **10**, 77 (1985).
[23] R. S. Weis and T. K. Gaylord, Appl. Phys. **A 37**, 191 (1985).
[24] W. Bollmann, K. Schlothauer, and J. Zogal, Krist. Techn. **11**, 1327 (1976).
[25] W. K. Lee, A. Nowick, and L. A. Boatner, Adv. Ceram. **23**, 378 (1987).
[26] L. Kovàcs, Zs. Szaller, I. Cravero, I. Földvri, and C. Zaldo, J. Phys. Chem. Solids **51**, 417 (1990).
[27] J. R. Herrington, B. Dischler, A. Räuber, and J. Schneider, Solid State Commun. **12**, 351 (1973).
[28] J. C. Owrutsky, N. H. Rosenbaum, L. M. Tack, and R. J. Saykally, J. Chem. Phys. **783**, 5338 (1985).
[29] J. B. Bates and R. A. Perkins, Phys. Rev. B **16**, 3713 (1977).
[30] G. Herzberg, *Molecular Spectra and Molecular Structure 1: Spectra of Diatomic Molecules* (Van Nostrand, New York, 1950), Chap. 3.
[31] B. Wedding and M. V. Klein, Phys. Rev. **177**, 1274 (1969).
[32] P. E. Cade, J. Chem. Phys. **47**, 2390 (1967).
[33] L. Kovàcs, M. Wöhlecke, A. Jovanovic, K. Polgar, and S. Kapphan, J. Phys. Chem. Solids **52**, 797 (1991).
[34] R. Gonzalez, Y. Chen, K. L. Tsang, and G. P. Summers, Appl. Phys. Lett. **41**, 739 (1982).
[35] P. G. Johannsen, V. Schäferjohann, and S. Kapphan, private communication (unpublished).
[36] A. Gröne, M. Wöhlecke, and S. Kapphan (unpublished).
[37] J. B. Bates, J. C. Wang, and R. A. Perkins, Phys. Rev. B **19**, 4130 (1979).
[38] N. Schmidt, K. Betzler, M. Grabs, S. Kapphan, and F. Klose, J. Appl. Phys. **65**, 1253 (1989).
[39] S. Klauer, M. Wöhlecke and S. Kapphan, Radiat. Eff. Def. Solids **5**, 119 (1991); **5**, 699 (1991).